Available online at www.sciencedirect.com

ScienceDirect

Biochimica et Biophysica Acta 1768 (2007) 2409–2420

Biochimica et Biophysica Acta BBA

www.elsevier.com/locate/bbamem

Two-dimensional infrared correlation spectroscopy study of the interaction of oxidized and reduced cytochrome *c* with phospholipid model membranes

Angela Bernabeu [a], Lellys M. Contreras [b], José Villalaín [a,*]

[a] *Instituto de Biología Molecular y Celular, Universidad "Miguel Hernández", E-03202 Elche-Alicante, Spain*
[b] *Facultad de Ciencias y Tecnología, Universidad de Carabobo, Valencia, Venezuela*

Received 5 March 2007; received in revised form 18 April 2007; accepted 3 May 2007
Available online 22 May 2007

Abstract

We have used two-dimensional infrared correlation spectroscopy (2D-IR) to study the interaction and conformation of cytochrome *c* in the presence of a binary phospholipid mixture composed of a zwitterionic perdeuterated phospholipid and a negatively-charged one. The influence of the main temperature phase transition of the phospholipid model membranes on the conformation of cytochrome *c* has been evaluated by monitoring both the Amide I′ band of the protein and the CH_2 and CD_2 stretching bands of the phospholipids. Synchronous 2D-IR analysis has been used to determine the different secondary structure components of cytochrome *c* which are involved in the specific interaction with the phospholipids, revealing the existence of a specific interaction between the protein with cardiolipin-containing vesicles but not with phosphatidic acid-containing ones. Interestingly, 2D-IR is capable of showing the existence of significant changes in the protein conformation at the same time that the phospholipid transition occurs. In summary, 2D-IR revealed an important effect of the phospholipid phase transition of cardiolipin on the secondary structure of oxidized cytochrome *c* but not to either reduced cytochrome *c* or in the presence of phosphatidic acid, demonstrating the existence of specific intermolecular interactions between cardiolipin and cytochrome *c*.

Keywords: Cardiolipin; Cytochrome *c*; Phosphatidic acid; Two-dimensional infrared spectroscopy; Protein–lipid interaction

1. Introduction

Cytochrome *c* is a basic protein that has an essential role in the electron transport chain of eukaryotes. It performs its function by reversibly binding with its redox partners integrated into mitochondrial membranes and diffusing freely in the mitochondrial intermembrane space. This small peripheral protein acts as an electron transfer on the inner mitochondrial membrane surface where it is suggested to be partially inserted, at least in some steps during the electron transport, which could give rise to hydrophobic interactions with the membrane lipids [1,2]. Cytochrome *c* has been considered as a paradigm for electrostatically interacting peripheral membrane proteins since it is dissociated from lipid membranes by increasing ionic strength [3]. Many studies have shown its ability to bind and interact with anionic phospholipids and particularly with cardiolipin: the denaturation temperature of cytochrome *c* is decreased in their presence, they induce the appearance of infrared bands characteristic of aggregated proteins and increase its amide hydrogen–deuterium exchange rates, cytochrome *c* tends to aggregate at the lipid surface and induce the presence of non-bilayer structures, etc. [4–7].

Among the different phospholipids found in the mitochondrial membranes, cardiolipin, localized in the inner mitochondrial membrane, is the specific phospholipid required for a correct function of the electron transport in the mitochondria [8]. To this respect it is important to point that cardiolipin is a structurally unique phospholipid which contains two phosphate groups, four acyl chains, and is capable of forming intramolecular hydrogen bonding [9]. Many studies in lipid vesicle models have shown that cardiolipin and cytochrome *c* interact strongly

Abbreviations: 2D-IR, Two-dimensional infrared spectroscopy; DMPA, 1,2-Dimyristoyl-*sn*-Glycero-3-Phosphate; $DMPC_d$, 1,2-Dimyristoyl-d_{54}-*sn*-Glycero-3-Phosphocoline; MLV, Multilamellar vesicles; TMCL, 1,1′,2,2′-Tetramyristoyl-Cardiolipin; T_m, Temperature of the gel-to–liquid crystalline phase transition; IR, Infrared spectroscopy

* Corresponding author. Tel.: + 34 966 658 762; fax +34 966 658 758.
E-mail address: jvillalain@umh.es (J. Villalaín).

0005-2736/$ - see front matter © 2007 Elsevier B.V. All rights reserved.
doi:10.1016/j.bbamem.2007.05.002

with each other inducing conformational changes in the protein as well as in the phospholipids [3,7,10–15]. Cytochrome *c* interacts with cardiolipin-containing membranes largely by electrostatic interactions when the protein is in the native state, though the unfolded form seems to bind to membranes mainly by hydrophobic interactions [16,17]. The physiological consequences of the cytochrome *c* association with cardiolipin are not only restricted to its function as a component of the mitochondrial respiratory chain, but are also connected with the recently discovered ability of this protein to trigger programmed cell death (apoptosis), involving probably the cytochrome *c* release from its complexes with cardiolipin [10,18]. The release of cytochrome *c* from mitochondria followed by its binding to APAF1 constitutes a critical point of "no return" in the execution of the apoptotic program. Recently, it has been demonstrated that at early stages of apoptosis, cytochrome *c* bound to cardiolipin-containing mitochondrial membranes acts as a peroxidase that selectively catalyzes cardiolipin peroxidation, contributing to the outer mitochondrial membrane permeation, release of cytochrome *c* into the cytosol, and initiation of the apoptotic program [18–20].

Fourier transform infrared spectroscopy (FTIR) is a very well-suited technique to investigate the conformation of proteins because the analysis of the Amide bands provides information about their secondary structure. The Amide I band, in particular, which is mainly due to the carbonyl stretching vibration of the peptide bond, has been used extensively to determine the secondary structure of many proteins, both in free solution as well as associated to membranes by decomposition of the original Amide I band into its components and their posterior assignment and quantification [21,22]. However, due to the intrinsic bandwidth of the component bands, they highly overlap, making their identification very difficult. Recently, multidimensional IR spectroscopy methods have been applied to spread out congested spectra into a second dimension, such as non-linear two-dimensional infrared spectroscopy and two-dimensional infrared correlation spectroscopy [23–25]. Time-dependent variations in infrared spectra can be induced by an external perturbation (mechanical, thermal, chemical, etc.) and a correlation analysis of these fluctuations generates two-dimensional maps increasing the spectral resolution by spreading out peaks along the second dimension and revealing the order of the actual sequence of processes induced by the perturbation. This method provides a way to deconvolve amide bands into their secondary structure components, as well as to obtain the correlation of the interaction involving different elements pertaining to the same or different types of molecules in the same sample. 2D-IR has been applied to the study of different key aspects of proteins, such as the identification of their secondary structure components, aggregation, dynamics, denaturation, unfolding as well as protein–lipid interactions [26–30]. Herein, we report the results of our study using the generalized 2D-IR correlation procedure in order to investigate the interaction and conformation of cytochrome *c*, in both redox states, bound to phospholipid model membranes composed of binary mixtures of a zwitterionic phospholipid (perdeuterated dimyristoyl-*sn*-glycero-3-phosphate, $DMPC_d$) and a negatively charged one, either tetramyristoyl-cardiolipin (TMCL) or dimyristoyl-*sn*-glycero-3-phosphate (DMPA). The information on the protein secondary structure has been obtained both before and after the phase transition of the phospholipid binary mixtures. This approach provided a sensitive mean to detect minor structural changes in response to the phase transition of the phospholipid mixture due to temperature. Our analysis presents a direct evidence of the specific interaction between cytochrome *c* and cardiolipin, demonstrating the existence of significant interactions between different secondary structure elements of cytochrome *c* with this special type of phospholipid as well as the capability of this technique to study lipid–protein interaction.

2. Materials and methods

2.1. Materials

Bovine cytochrome *c* (type VI, oxidized form), deuterium oxide (99.9%), EDTA and HEPES were purchased from Sigma Chemical Co. (Madrid, Spain). Cytochrome *c* was used without any further purification. 1,2-Dimyristoyl-d_{54}-*sn*-Glycero-3-Phosphocoline ($DMPC_d$), 1,2-Dimyristoyl-*sn*-Glycero-3-Phosphate (DMPA) and 1,1′,2,2′-tetramyristoyl-cardiolipin (TMCL) were obtained from Avanti Polar Lipids (Alabaster, AL). Salts were of analytical grade. Water was twice distilled and deionized in a Millipore system from Millipore Ibérica (Madrid, Spain).

2.2. Sample preparation

Aliquots containing 3 mg of lipid in chloroform/methanol (2:1, v/v) were placed in a test tube, the solvents removed by evaporation under a stream of O_2-free nitrogen and finally, traces of solvents were eliminated under vacuum in the dark for more than 3 h. The molar relationship between phospholipids in the mixtures was 2:1 for both $DMPC_d$/TMCL and $DMPC_d$/DMPA. A pre-weighted amount of freeze-dried protein was suspended by addition of an appropriate volume of 20 mM HEPES, 50 mM NaCl, 0.1 mM EDTA, pH* 7.4 buffer in D_2O, to give a final concentration of about 10 mM. The protein solution was then added to the tube containing the dried lipid to obtain a final lipid/protein mole ratio of 25:1, and the suspension was vortexed at about 5 °C above the transition temperature of the phospholipid mixture to obtain multilamellar vesicles (MLV). The mixture was freezed/thawed twice in order to ensure a complete homogeneity of the sample and maximization of contacts between the protein and the phospholipid and then incubated for 10 min at 5 °C above the transition temperature with occasional vortexing. The freeze/thaw cycle was repeated again and the suspension was then centrifuged at 10000 rpm for 20 min in order to remove the protein that was not bound to the phospholipid in the membrane. The freeze/thaw, incubation and centrifugation steps were repeated twice more in order to remove the unbound protein. The pellet was resuspended in D_2O buffer and used for the measurements. This process ensured that the H–D exchange was maximized. When required, reduced cytochrome *c* was obtained by incubation of oxidized cytochrome *c* with a buffer solution containing a small quantity of dithionite. Afterwards reduced cytochrome *c* was passed through a column containing G-25 Sephadex in order to remove the dithionite. The reduced cytochrome *c*ontaining solution was lyophilized, checked for the reduction extent and used immediately afterwards to prepare the samples as stated above. The phospholipid and peptide concentration were measured by methods described previously [31,32]. The final lipid/protein ratio, measured by comparison of the lipid C═O stretch/Amide I ratios obtained before and after centrifugation, was about 55:1 and 58:1 for oxidized cytochrome *c* and about 54:1 and 61:1 for reduced cytochrome *c* in the presence of the phospholipid mixtures $DMPC_d$/TMCL and $DMPC_d$/DMPA, respectively.

2.3. Infrared spectroscopy

For the infrared measurements, MLVs, resuspended in approximately 25 μl of D_2O buffer, were placed in between two CaF_2 windows separated by 50 μm

Teflon spacers and transferred to a Harrick Ossining demountable cell. Fourier transform infrared spectra were obtained in a Nicolet 520 Fourier transform infrared spectrometer equipped with a DTGS detector. Each spectrum was obtained by collecting 250 interferograms with a nominal resolution of 2 cm^{-1} and then Fourier transformed using a triangular apodization. A sample shuttle accessory was used in order to average background spectra between sample spectra over the same time period. The spectrometer was continuously purged with dry air at a dew point of −40 °C in order to remove atmospheric water vapor from the bands of interest and avoid correlation peaks due to the water vapor. The spectra were recorded after equilibrating the samples at 8 °C for 20 min in the infrared cell at 2 °C intervals with a 2-min delay between each scan using an external bath circulator connected to the infrared spectrometer. Subtraction of buffer spectra taken at the same temperature as the samples was performed interactively using either Grams or Spectra-Calc (Galactic Industries, Salem, NH) as described previously [33]. Frequencies at the centre of gravity, when necessary, were measured by taking the top 10 points of each specific band and fitted to a Gaussian band. Band-narrowing strategies were applied in order to resolve the component bands in the Amide I′ region, i.e., derivation and Fourier self-deconvolution [34,35]. Second-derivative spectra were calculated over a 15-data point range. Fourier self-deconvolution was done using the deconvolution software of Grams, which uses the deconvolution technique of Griffiths and Pariente, with a narrowing parameter (γ) of 7.8 and a smoothing parameter of 80% [36]. These parameters assumed that the spectra were not over-deconvolved as was evidenced by the absence of negative side lobes. Protein secondary structure elements were quantified from curve-fitting analysis by band decomposition of the original Amide I′ band after spectral smoothing using the same software stated above [33]. Briefly, for each component, three parameters were considered: band position, band height and band width. The number and position of component bands was obtained through deconvolution and in decomposing the amide I′ band, Gaussian components were used. The curve-fitting procedure was accomplished in two steps: in the first one, band position was fixed, allowing width and heights to approach final values, and in the second one, band positions were left to change. When necessary, these two steps were repeated. Band decomposition was performed using SpectraCalc (Galactic Industries, Salem, MA). The fitting result was evaluated visually by overlapping the reconstituted overall curve on the original spectrum and by examining the residual obtained by subtracting the fitting from the original curve. The procedure gave differences of less than 2% in band areas after the artificial spectra were submitted to the curve fitting procedure. The frequency positions of the band centers were independently evaluated by second derivative procedures, being always very close to the positions found by deconvolution. It is assumed that the extinction coefficients of the different protein components do not differ to a great extent and that the error derived from this assumption is within the range of errors inherent to the methodology.

2.4. Two-dimensional correlation infrared spectroscopy

Two-dimensional correlation analysis was carried out using the 2D-Shige program written by Shigeaki Morita and Yukihiro Ozaki (Kwansei-Gakuin University, Japan) obtained from the webpage http://sci-tech.ksc.kwansei.ac.jp/~ozaki/e_2D.htm. To obtain the 2D-IR maps, heating was used as the perturbation to induce time-dependent spectral fluctuations in the IR spectra of $DMPC_d$/TMCL/cytochrome *c* and $DMPC_d$/DMPA/cytochrome *c* complexes, in both the oxidized and reduced states, so that to induce the phase transition of the phospholipid membranes and observe any modulation of the conformation on the protein induced by the phase change. Correlation intensities were computed for the infrared spectra at different temperatures by applying the generalized two-dimensional correlation algorithm of Noda through the 2D-Shige program. The average spectra of the temperature scans were used as reference in the analysis. Although it was possible to obtain 2D correlation plots from the original spectra, the spectra selected for the correlation analysis were Fourier self-deconvolved before the actual analysis was performed [37]. The absence of artifacts in the deconvolved spectra was verified by comparing and confirming that the number of bands and their positions arising in the deconvolved spectra matched those in obtained in the second-derivative spectra [38]. Visualization of the 2D-IR maps was performed with the use of Origin software (Microcal Systems, Boulder, CO). The maximum and minimum intensities for the whole correlation map were found, their values were multiplied by two and a maximum of thirty contour lines were drawn, so that the number of contour lines reflect their intensities in relation to the main peak. As reviewed by Noda [25], the synchronous (in our case, synthermal) 2D correlation spectrum of dynamic spectral intensity variations represents the simultaneous occurrence of coincidental changes in spectral intensities measured at frequencies *v*1 and *v*2. The asynchronous (in our case, asynthermal) spectrum of dynamic spectral intensity variations represents sequential, or unsynchronized, changes in spectral intensities measured at *v*1 and *v*2. In the synchronous spectrum correlation peaks appear at both diagonal and off-diagonal peaks (auto-peaks and cross-peaks, respectively), whereas the asynchronous spectrum has no auto-peaks, but cross-peaks located at off-diagonal positions. Since the synchronous spectrum is always required for interpretation of intensity and width changes, and our interest aims to find the inter-molecular interactions between cytochrome *c* and the phospholipid molecules, we have used throughout this work the synchronous 2D-IR correlation contour maps to analyze the data as it has been done before [39].

3. Results

3.1. Thermotropic behavior of the phospholipids in the binary mixtures

We have studied by infrared spectroscopy the binding and interaction of both oxidized and reduced cytochrome *c* with two different binary phospholipid mixtures, namely $DMPC_d$/TMCL and $DPMC_d$/DMPA, in order to observe any effect on both types of molecules, phospholipid and protein. It is well established that a shift in the frequency of the CH_2 symmetric stretching band is a reliable index of the phase behavior of a phospholipid dispersion, since the CH_2 stretching frequencies respond primarily to conformational disorder and increase with the introduction of *gauche* bonds in the fatty acyl chains [40]. Since in this study one of the phospholipids was acyl chain-perdeuterated ($DMPC_d$), and the other was not, it was possible to independently detect changes which might occur with each one (3000–2800 cm^{-1} and 2200–2000 cm^{-1} regions, Fig. 1). Moreover, since the samples have been prepared by mixing and washing the unbound protein as described in Materials and methods, the data correspond to the phospholipid acyl chains when the protein was effectively bound to the phospholipid membrane.

The temperature dependence of the CH_2 and CD_2 symmetric stretching frequencies in the absence of cytochrome *c* of TMCL and $DMPC_d$ in the $DMPC_d$/TMCL 2:1 mixture are shown in Fig. 2A, whereas the temperature dependence of the CH_2 and CD_2 symmetric stretching frequencies of DMPA and $DMPC_d$ in the

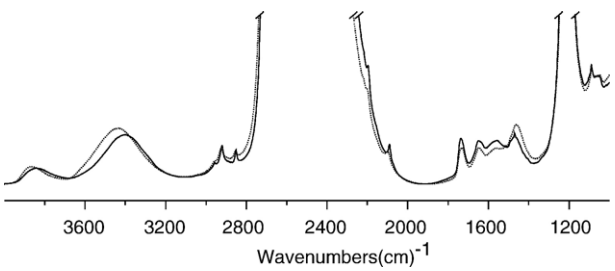

Fig. 1. Infrared spectra in the 4000–1000 cm^{-1} range for the sample containing oxidized cytochrome *c* and the phospholipid mixture DMPCd/TMCL at 20 °C (—) and 70 °C (·····).

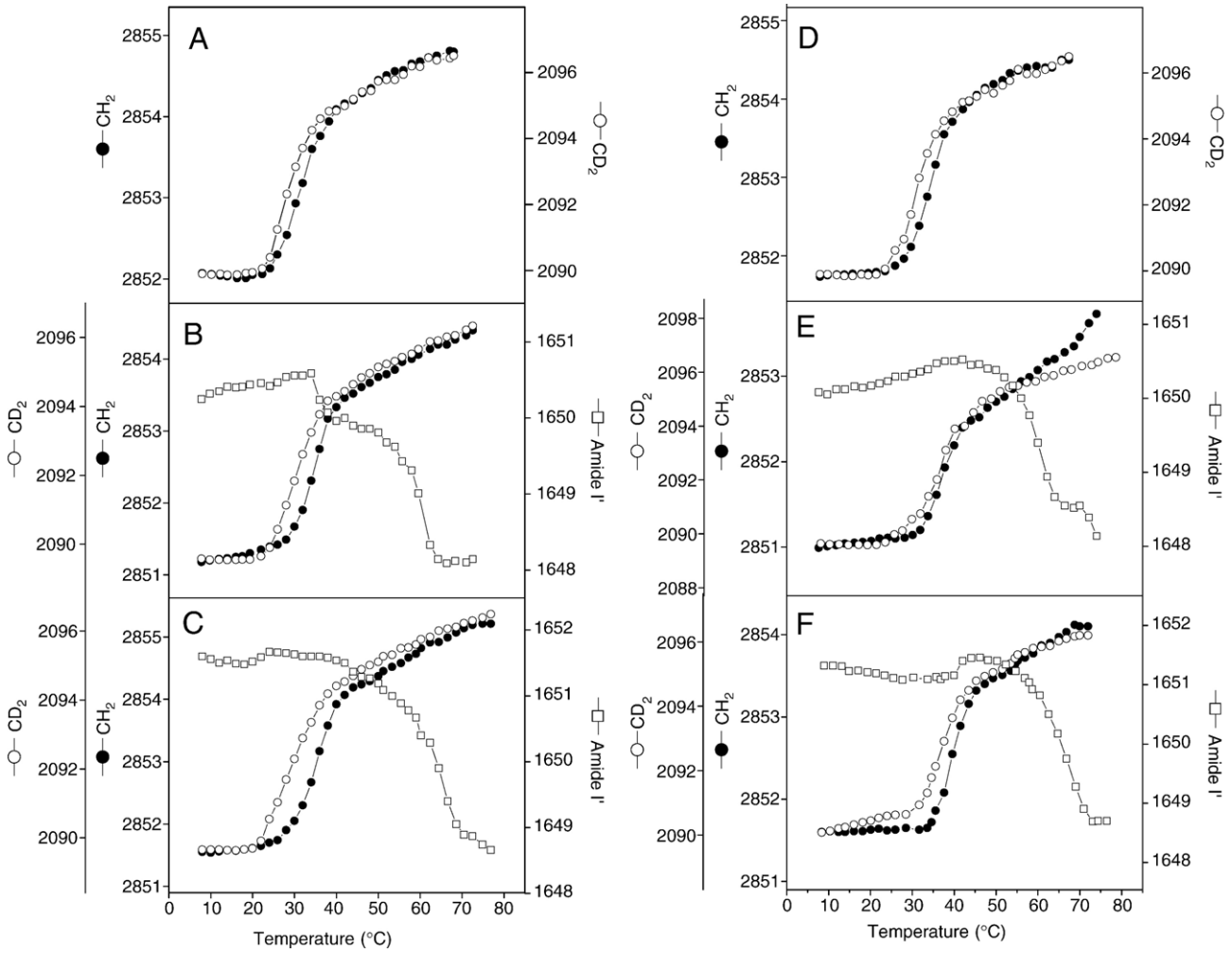

Fig. 2. Frequency of the symmetrical CH2 stretching (●), the symmetrical CD2 stretching (○) and the maximum of the Amide I′ band of cytochrome *c* (□) for mixtures containing DMPCd/TMCL (A–C) and DMPCd/DMPA (D–F) at a molar relationship of 2:1 as a function of temperature in the absence (A, D) and in the presence of cytochrome *c* (B, C, E and F) in the oxidized (B, E) and reduced forms (C, F).

$DMPC_d$/DMPA 2:1 mixture are shown in Fig. 2D. In the absence of cytochrome *c*, the observed transitions, which correspond to the gel-to-liquid crystalline phase transition for both mixtures $DMPC_d$/TMCL and $DMPC_d$/DMPA, were slightly broad, showing T_m values between the ones observed for the pure phospholipids (T_m is approximately 20 °C for $DMPC_d$ [41], 34 °C for TMCL [42] and 50 °C for DMPA [43]). The slightly broadening which is observed could be related to a non-ideal behavior of the phospholipid mixtures, but no evidence for domain formation is apparent [44]. The mean T_m values were 27 °C for $DMPC_d$ and 31 °C for TMCL in the $DMPC_d$/TMCL mixture, and 31 °C for $DMPC_d$ and 34 °C for DMPA in the $DMPC_d$/DMPA mixture. When oxidized and reduced cytochrome *c* were present in the binary mixture composed of $DMPC_d$/TMCL, similar transitions were observed (Fig. 2B and C, respectively) but they showed small shifts to higher temperatures (about 2–3 °C) in their T_m values. These T_m values were 29 °C for $DMPC_d$ and 34 °C for TMCL in the presence of oxidized cytochrome *c* and 29 °C for $DMPC_d$ and 35 °C for TMCL in the presence of reduced cytochrome *c*. When oxidized and reduced cytochrome *c* were present in the binary mixture composed of $DMPC_d$/DMPA, a similar effect was found since the T_m values were shifted to higher temperatures (about 2–5 °C) with respect to the T_m values in the absence of the protein (Fig. 2E and F, respectively). These T_m values were 33 °C for $DMPC_d$ and 37 °C for DMPA in the presence of oxidized cytochrome *c* and 36 °C for $DMPC_d$ and 39 °C for DMPA in the presence of reduced cytochrome *c*. It is interesting to note that the difference between the T_m of each specific phospholipid in the same mixture was slightly higher for the $DMPC_d$/TMCL mixture than for the $DMPC_d$/DMPA one.

3.2. Secondary structure of cytochrome c in the presence of the phospholipid model membranes

The infrared spectra of the Amide I′ region of fully hydrated cytochrome *c* in D_2O buffer at 20 °C and 70 °C in the oxidized and reduced forms, both in free solution and bound to either $DMPC_d$/TMCL or $DMPC_d$/DMPA binary mixtures, are shown in Fig. 3. The spectra is formed by different underlying components, appearing at about 1686, 1672, 1655, 1643, 1632, and 1617 cm^{-1} as observed by self-deconvolution and derivation, in

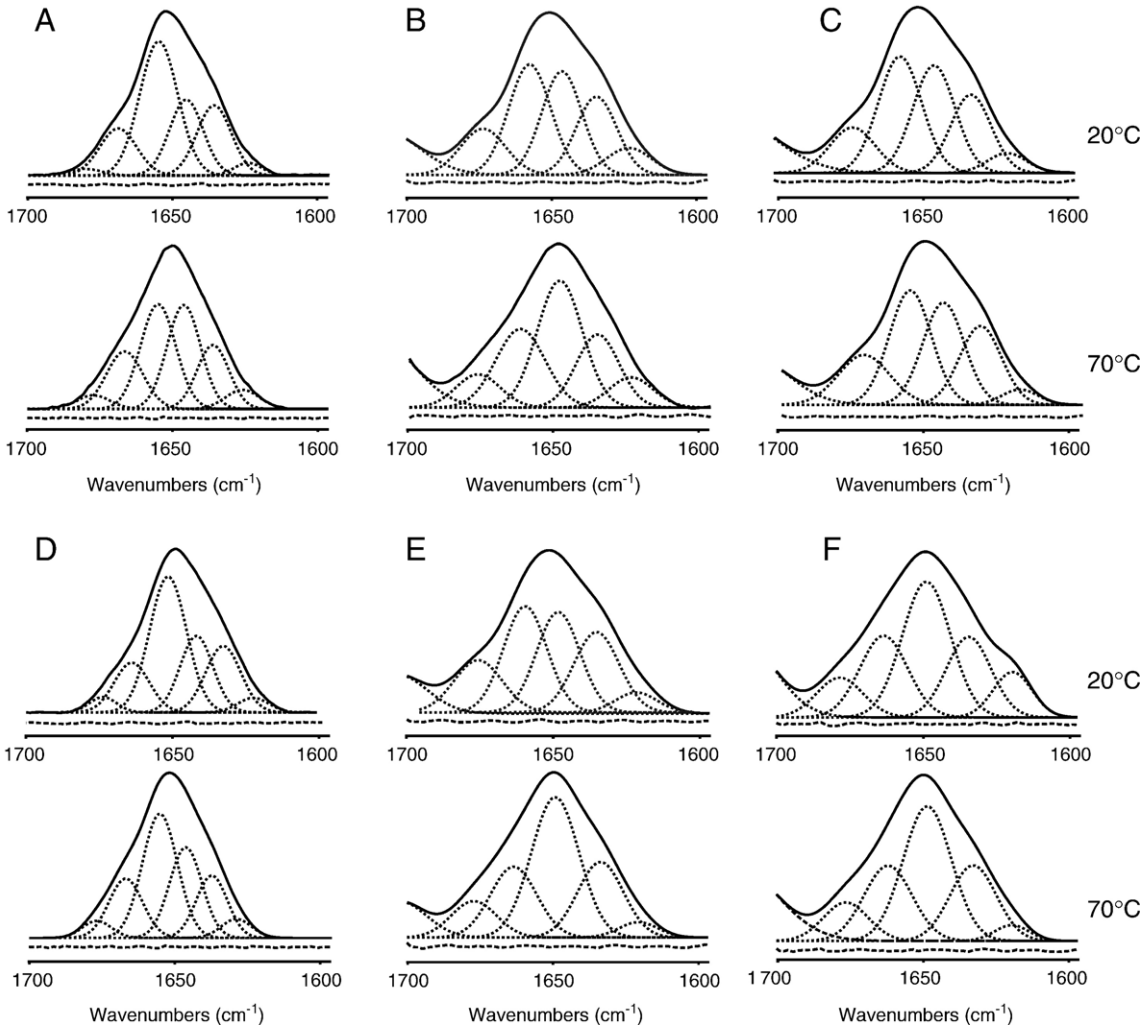

Fig. 3. Amide I′ band decomposition of cytochrome *c* in solution (A, D) and in the presence of phospholipid binary mixtures composed of DMPCd/TMCL (B, E) and DMPCd/DMPA (C, F) model membranes at a molar relationship of 2:1. Cytochrome *c* was either oxidized (A–C) or reduced (D–F). The component bands (dotted line), the original envelope (solid line) and the difference between the fitted curve and the original spectrum (dashed line) are shown. The spectra shown were obtained at 20 °C and 70 °C as indicated in the figure.

agreement with previous reports [6,28,29,45]. To assign the component bands to specific structural features and estimate the percentage of each component, we have decomposed the Amide I′ infrared band as described in Materials and methods and compared them to literature values [22]. For cytochrome *c* in solution, the component at 1655 cm^{-1}, the main one, is characteristic of -helices [46] while the components at 1672 cm^{-1} and 1632 cm^{-1} are generally associated with β-turns and β-sheets, respectively. However, these bands have been also attributed to extended chains connecting α-helices [47], to helix-helix interactions [48] as well as to solvent accessible helices [49]. Since cytochrome *c* is composed of three major and two minor -helices [50] and contain little β-structure [51] we have assigned the bands appearing at 1655 and 1632 cm^{-1} to α-helices [49]. Taking into account all these data, the secondary structure content of cytochrome *c* in solution is presented in Table 1. At 20 °C, both the oxidized and reduced forms of cytochrome *c* present a similar secondary structure content, being the α-helix the greatest one, in accordance with previous results [52–54]. Upon increasing the temperature (see Table 1), the α-helical content decreased at the same time that random and β-turn structures increased for both redox states of cytochrome *c* in accordance with previous results [6,28,45]. However, the extent of the change was greater for the oxidized form that for the reduced form, indicating that the reduced form is more stable thermally than the oxidized one [55].

Upon binding of cytochrome *c* to vesicles composed of either $DMPC_d$/TMCL or $DMPC_d$/DMPA both at a 2:1 molar ratio (Fig. 3), the Amide I′ band maximum was shifted about 2–3 cm^{-1} towards lower wavenumbers, either in the gel or in the liquid–crystalline phases, in agreement with previous results [6, 29]. The number of the Amide I′ component bands were identical to those found for the protein in solution, but their frequency and intensity was not (Fig. 3 and Table 1). Whereas both oxidized and reduced forms of cytochrome *c* in the presence of either $DMPC_d$/TMCL or $DMPC_d$/DMPA, presented similar secondary structure contents at 20 °C, they showed different secondary structure contents compared to the protein in solution. In the

Table 1
Comparison of the secondary structure content of cytochrome *c* as determined by infrared spectroscopy in solution and in the presence of phospholipid binary mixtures as indicated (see text for details).

	T (°C)	α-Helix/3_{10}-Helix 1650–1670 cm^{-1}/ 1625–1640 cm^{-1}	Random 1641– 1649 cm^{-1}	β-Turn 1670– 1690 cm^{-1}
Solution	Ox 20	63%	21%	16%
	Ox 70	48%	30%	22%
	Rd 20	61%	21%	18%
	Rd 70	54%	25%	21%
+$DMPC_d$/TMCL 2:1	Ox 20	55%	30%	15%
	Ox 70	49%	41%	10%
	Rd 20	51%	34%	15%
	Rd 70	45%	44%	11%
$DMPC_d$/DMPA 2:1	Ox 20	52%	29%	19%
	Ox 70	48%	41%	11%
	Rd 20	54%	29%	17%
	Rd 70	47%	43%	10%

The values are rounded off to the nearest integer.
Ox/Rd, oxidized and reduced cytochrome *c*, respectively.

presence of the binary phospholipid mixtures and for both redox forms of cytochrome *c*, while the intensity of the α-helical component decreased about 10%, the random component increased about the same extent, the content of β-turns remaining very similar (Table 1). At 70 °C, while the α-helical and β-turn content decreased, the random coil increased (Table 1). These data demonstrate that both oxidized and reduced forms of bovine cytochrome *c* interact with membranes containing negatively-charged phospholipids as well as the secondary structure of the protein changes upon this interaction. Interestingly, when pure $DMPC_d$ was used to form the model membranes, the protein was recovered almost completely in the supernatant (not shown), demonstrating therefore that the protein only binds to negatively-charged membranes. It should also be noted that the deuteration level of cytochrome *c* was maximized for all samples (see Materials and methods), since the intensity of the Amide II band of cytochrome *c* in all samples was minimal; furthermore, the observed changes in the Amide II envelope were insignificant and ascribed to denaturation of the protein at high temperatures (not shown for briefness). It is interesting to note that the denaturation temperature of cytochrome in solution is about 80 °C [6] but 20–30 °C lower when bound to vesicles of pure anionic phospholipids [6,29,45].

In Fig. 4 we present the stacked infrared difference spectra of the C═O and Amide I′ regions at different temperatures of mixtures containing either oxidized or reduced cytochrome *c* with either $DMPC_d$/TMCL or $DMPC_d$/DPMA binary mixtures. For the sample containing oxidized cytochrome *c* in the presence of the $DMPC_d$/TMCL mixture (Fig. 4A) it is possible to observe two different transitions, one defined by the change in the intensity of the C═O component band of the phospholipid mixture, appearing at about 1737 cm^{-1}, and another one defined by the change in the intensity of well defined Amide I′ components appearing at about 1670, 1656 and 1633 cm^{-1} (note the differences in intensities). The main change in the intensity of the 1737 cm^{-1} band occurs at about 28–32 °C whereas the change in the intensity of the protein bands occur at about 59–61 °C, i.e., the first one coincides with the T_m of the phospholipid mixture and the second one coincides with the denaturation temperature of the protein. However, small but significant changes in intensity were observed in the Amide I′ components at temperatures in which the T_m occurs. Therefore, the changes we observe in this mixture correlate very well with the changes in secondary structure commented above. Similar results were observed for the other mixtures (Fig. 4B–D) since transitions about 27–34 °C and 63–65 °C were obtained for the mixture of reduced cytochrome *c* in the presence of $DMPC_d$/TMCL, about 34–36 °C and 59–60 °C were obtained for the mixture of oxidized cytochrome *c* in the presence of $DMPC_d$/DPMA, and about 35–39 °C and 64–66 °C were obtained for the mixture of reduced cytochrome *c* in the presence of $DMPC_d$/DPMA.

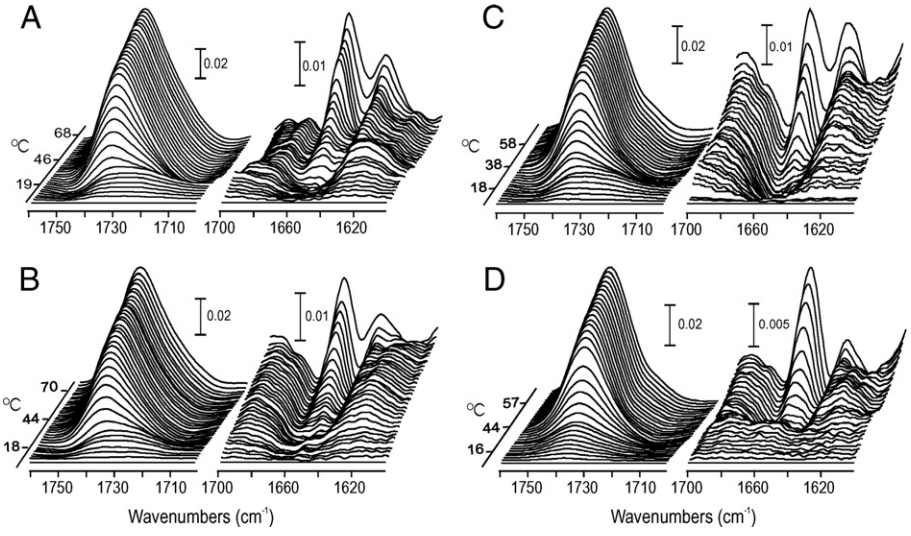

Fig. 4. Stacked difference infrared spectra of the C═O and Amide I′ regions of the mixture DMPCd/TMCL plus oxidized (A) and reduced (B) cytochrome *c* and the mixture DMPCd/DPMA plus oxidized (C) and reduced (D) cytochrome *c* recorded at regularly increasing temperature intervals as indicated. The first spectrum was taken as the reference one. The vertical bars represent absorbance units as indicated.

3.3. Two-dimensional correlation analysis of oxidized and reduced cytochrome c

The above mentioned data cannot provide information on the interactions between the secondary-structure elements of the protein and the phospholipids that give rise to the observed changes. We have therefore used 2D-IR in order to get a deeper insight on the interaction between the phospholipids in the different mixtures and cytochrome *c* in its two redox states. Since, as shown above, there are two transitions when cytochrome *c* is mixed with either $DMPC_d$/TMCL or $DMPC_d$/DPMA, the first one corresponding to the gel to liquid–crystalline phase transition of the phospholipids and the second one to the unfolding of the protein due to its denaturation, we have obtained 2D-IR correlation maps at two temperature ranges, the first one encompassing the gel to liquid–crystalline phase transition of the phospholipid mixture and the second one encompassing the denaturation of the protein (see Fig. 2).

The 2D-IR analysis of oxidized and reduced cytochrome *c* in buffer at two temperature ranges is shown in Fig. 5. The synchronous 2D-IR correlation contour map of oxidized cytochrome *c* corresponding to heating from 12 °C to 52 °C (Fig. 5A) shows two main auto-peaks located at 1669 and 1645 cm^{-1} and a smaller auto-peak at 1623 cm^{-1}, indicating that

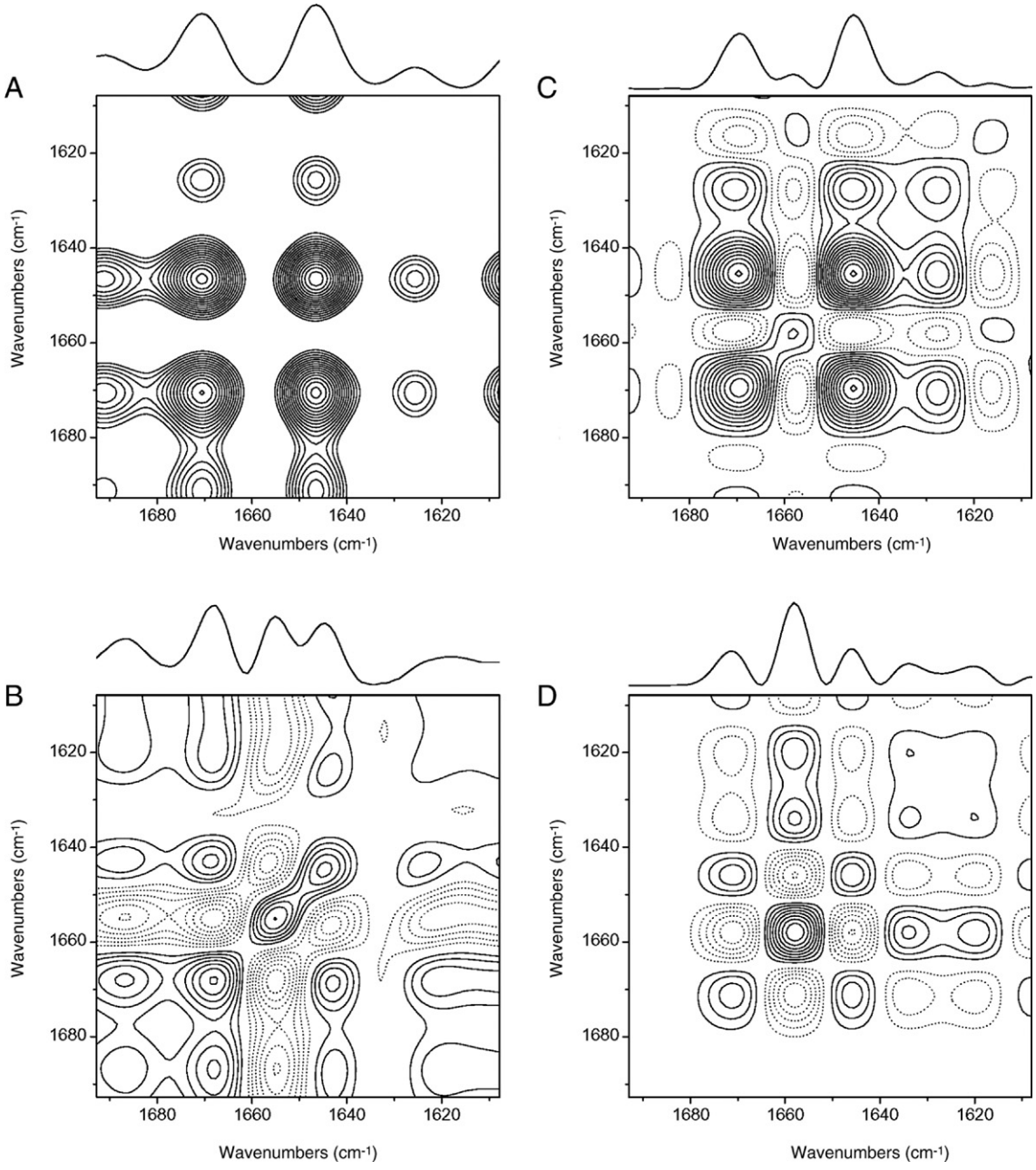

Fig. 5. Synchronous 2D-IR maps in the Amide I′ region of oxidized (A, B) and reduced (C, D) cytochrome *c* in D2O buffer as a function of temperature. The range of temperatures used for the generation of the 2D-IR maps were 12–52 °C (A), 52–78 °C (B) for the oxidized cytochrome *c*, and 12–62 °C (C) and 62–78 °C (D) for the reduced one. The correlation spectra were obtained using the 2D-Shige program. The solid and dotted lines represent positive and negative peaks, respectively. The spectra shown above the 2D-IR maps correspond to the diagonal auto-peaks.

these are the frequencies at which the main changes take place during this temperature range. It should be noted that frequencies above 1685 cm^{-1} and below 1620 cm^{-1} were not taken into account in order to obtain information about secondary structures since they are not related to specific secondary structure elements of proteins (see above). The most intense cross-peaks were observed at the same frequencies (1669–1645 cm^{-1}) and were positive, indicating that, during the heating process, these two components were synchronized. Smaller positive cross-peaks appeared at 1669–1623 cm^{-1} and 1645–1623 cm^{-1}. These observations emphasize that for the protein in solution and below its denaturation temperature, the major changes occur on bands corresponding to β-turns and random structures and to a lesser extent to α-helix. The synchronous 2D-IR correlation contour map of oxidized cytochrome *c* (52 °C to 78 °C, Fig. 5B), shows three main auto-peaks located at 1668, 1655 and 1643 cm^{-1}, indicating that these are the frequencies at which the main changes take place during this temperature range. The most intense cross-peaks were observed at frequencies 1668–1655 cm^{-1}, 1655–1642 cm^{-1} and 1668–1642 cm^{-1}. Whereas the two first cross-peaks were negative, indicating that, during the heating process, one increased while the other one decreased, the third one was positive, indicating that these two components were synchronized during denaturation. The synchronous 2D-IR correlation contour map of reduced cytochrome *c* corresponding to heating from 12 °C to 62 °C (Fig. 5C) shows two main auto-peaks located at 1669 and 1645 cm^{-1} similarly to the one corresponding to the oxidized form but two smaller auto-peaks at 1656 and 1626 cm^{-1}. The most intense cross-peak was observed at the same frequencies (1669–1645 cm^{-1}) and was positive. Smaller positive cross-peaks appeared at 1669–1626 cm^{-1} and 1645–1626 cm^{-1}. However, there were three less-intense negative cross-peaks at 1669–1657 cm^{-1}, 1657–1645 cm^{-1}, and 1657–1626 cm^{-1}, reflecting a different behavior to the oxidized form. The synchronous correlation map for reduced cytochrome *c* (62 °C to 78 °C, Fig. 4D) shows one main autopeak at 1657 cm^{-1} and smaller auto-peaks at 1670, 1645, 1633 and 1620 cm^{-1}, frequencies at which the main changes take place during this denaturation range. The most intense cross-peaks were observed at frequencies 1670–1657 cm^{-1}, 1657–1645 cm^{-1} and 1670–1645 cm^{-1}. Similarly to what was found for the oxidized form of cytochrome *c*, the two first cross-peaks were negative and the third one was positive. Small intensity cross-peaks appeared at 1657–1633 cm^{-1} and 1657–1620 cm^{-1} (positive) and 1670–1633 cm^{-1}, 1670–1620 cm^{-1}, 1645–1633 cm^{-1} and 1645–1620 cm^{-1} (negative). The data for both oxidized and reduced cytochrome *c* forms are fully consistent with previous IR data, i.e., the disappearance of the α-helix component is associated with the appearance of random structures during the unfolding process.

3.4. Two-dimensional correlation analysis of cytochrome c bound to membranes

The synchronous 2D-IR correlation contour map of oxidized cytochrome *c* in the presence of $DMPC_d$/TMCL corresponding to the temperature range from 8 to 46 °C (Fig. 6A) presents much less intense auto-peaks and cross-peaks than that corresponding to the phospholipid bands (not shown) because this range encompass the gel to liquid–crystalline phase transition. The most intense and narrow Amide I′ auto-peaks were located at 1658 and 1633 cm^{-1} indicating that these are the frequencies at which the main changes should take place due to the interaction of the protein with the phospholipids. Smaller intensity auto-peaks were observed at 1678, 1669 and 1616 cm^{-1} (peaks at frequencies higher than 1690 cm^{-1} are due to the deconvolution wings of the C═O band of the phospholipid). The most intense cross-peak was observed at the same frequencies (1658–1633 cm^{-1}) and it was positive. Less intense, but informative, cross-peaks were observed correlating frequencies 1678–1657 cm^{-1}, 1678–1633 cm^{-1}, 1678–1617 cm^{-1}, 1657–1617 cm^{-1} and 1633–1617 cm^{-1} (positive), as well as 1669–1657 cm^{-1} and 1669–1633 cm^{-1} (negative). These data indicate that the major secondary structure of the protein which more significantly senses the phase transition of the phospholipid mixture is the α-helix component (bands at 1658 cm^{-1} and 1633 cm^{-1}). When the synchronous 2D-IR correlation contour map was obtained for reduced cytochrome *c* in the presence of $DMPC_d$/TMCL (8 to 50 °C, Fig. 6B) there were wider and less intense auto-peaks and cross-peaks than those corresponding to the oxidized one. The major Amide I′ auto-peaks were located at 1635 and 1621 cm^{-1}, and minor ones were observed at 1681, 1671, 1658 and 1645 cm^{-1}. The secondary structure components which varied the most were the ones assigned to α-helix (1635 cm^{-1}) and aggregated β-sheet (1621 cm^{-1}). The appearance of small positive cross-peaks at 1681–1636 cm^{-1} and 1681–1622 cm^{-1} would indicate the appearance of small quantities of intermolecularly aggregated β-sheet. The synchronous 2D-IR correlation contour maps of oxidized and reduced cytochrome *c* in the presence of $DMPC_d$/DMPA corresponding to the temperature ranges from 12 to 48 °C and 12 to 51 °C are shown in Fig. 5C and D, respectively. Besides presenting much less intense and wider auto-peaks than the one observed for the oxidized form of cytochrome *c* in the presence of $DMPC_d$/TMCL but similar to the synchronous spectrum of reduced cytochrome *c*, it is noteworthy to observe that both correlation maps were nearly identical since broad auto-peaks were observed at about 1626 cm^{-1} and 1619 cm^{-1}.

The synchronous 2D-IR correlation contour map of oxidized cytochrome *c* in the presence of $DMPC_d$/TMCL corresponding to the temperature range from 48 to 73 °C presents higher intense auto-peaks and cross-peaks than that corresponding to the low temperature range (Fig. 6A). The most intense Amide I′ auto-peak was located at 1656 cm^{-1} and less intense but significant auto-peaks were found at 1667 and 1646 cm^{-1} as well as a small auto-peak at 1635 cm^{-1}. The most intense cross-peaks were observed at 1666–1646 cm^{-1} and 1656–1646 cm^{-1} (positive) as well as 1666–1656 cm^{-1} and 1656–1646 cm^{-1} (negative). Smaller negative cross-peaks appeared at 1666–1637 cm^{-1} and 1646–1637 cm^{-1} (negative). These data indicate that the major change which takes place for oxidized cytochrome *c* at this temperature range is due to unfolding. The synchronous 2D-IR correlation contour map obtained for

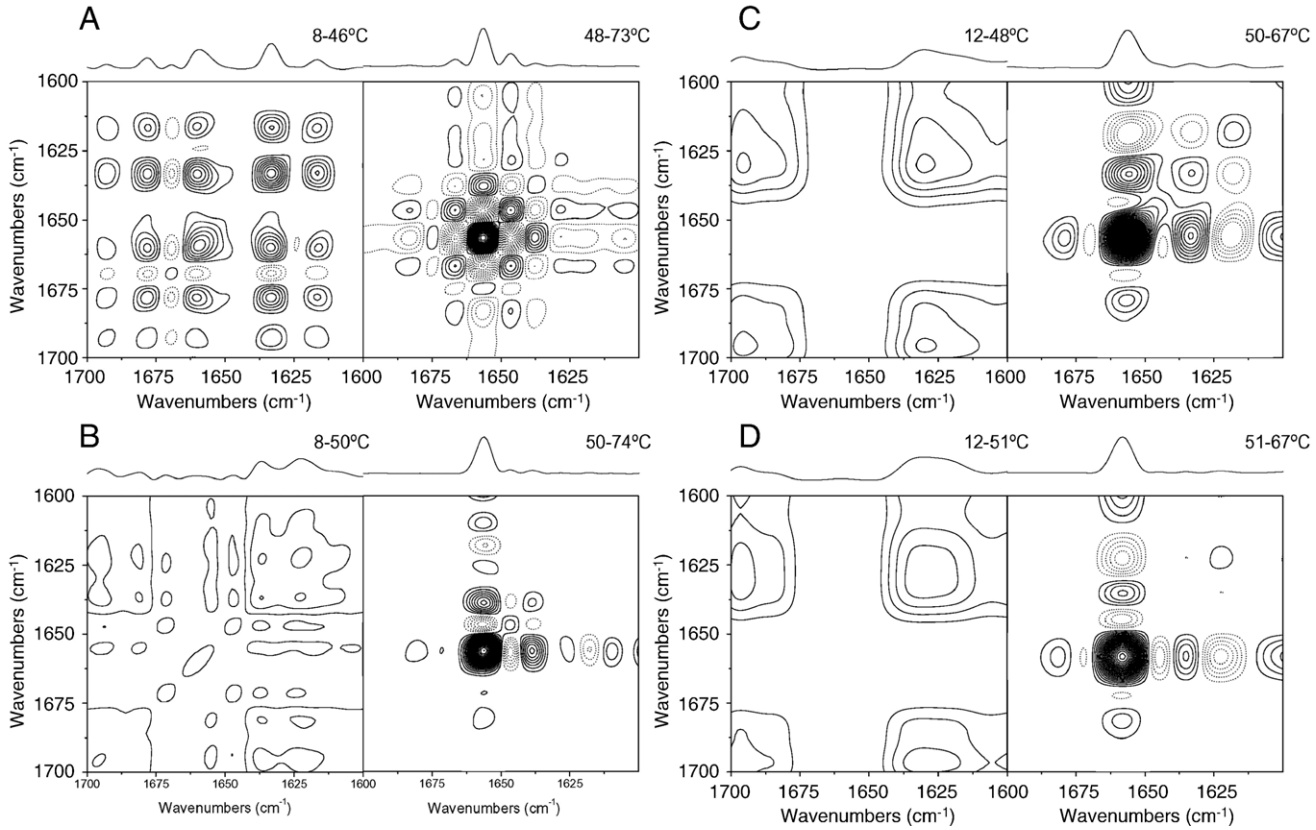

Fig. 6. Synchronous 2D-IR maps in the Amide I′ region of oxidized (A, C) and reduced (B, D) cytochrome *c* in the presence of binary phospholipid mixtures composed of DMPCd/TMCL (A, B) and DMPCd/DMPA (C, D) model membranes at a molar relationship of 2:1. The range of temperatures used for the generation of the 2D-IR maps were 8–46 °C and 48–73 °C (A), 8–50 °C and 50–74 °C (B), 12–48 °C and 50–67 °C (C) and 12–51 °C and 51–67 °C (D). The correlation spectra were obtained using the 2D-Shige program. The solid and dotted lines represent positive and negative peaks, respectively. The spectra shown above the 2D-IR maps correspond to the diagonal auto-peaks.

reduced cytochrome *c* in the presence of $DMPC_d$/TMCL at a temperature range from 50 to 74 °C (Fig. 6B) presented an intense Amide I′ auto-peak located at 1656 cm^{-1}, similarly to what was found for oxidized cytochrome *c*. Less intense auto-peaks were found at 1646 and 1637 cm^{-1}. The most intense cross-peak was found at 1656–1637 cm^{-1} (decrease in α–helix). Negative auto-peaks were found at 1656–1646 cm^{-1} and 1646–1637 cm^{-1} indicating that the decrease in α-helix was accompanied by an increase in random coil.

The synchronous 2D-IR correlation contour map of oxidized cytochrome *c* in the presence of $DMPC_d$/DMPA corresponding to the temperature range from 50 to 67°C (Fig. 6C) presents an intense auto-peak at 1656 cm^{-1} and less intense auto-peaks at 1644, 1634 and 1618 cm^{-1}. Differently to what was found for both oxidized and reduced cytochrome *c* in the presence of $DMPC_d$/TMCL, negative cross-peaks at 1656–1618 cm^{-1} and 1633–1618 cm^{-1} accompanied by a positive cross-peak at 1656–1634 cm^{-1} indicated that the decrease in α-helix was accompanied by a significant increase in aggregated intermolecular β-sheet. A small cross-peak at 1656–1644 cm^{-1} was also apparent, indicating that random structures increased at the same time that α-helix decreased. The 2D-IR correlation contour map of reduced cytochrome *c* in the presence of $DMPC_d$/DMPA at a temperature range from 51 to 67 °C (Fig. 6D) was very similar. The most intense Amide I′ auto-peak was located at 1656 cm^{-1} along with another small one at 1621 cm^{-1}. Again, the most intense cross-peak (negative) was found at 1655–1621 cm^{-1}, indicating that the increase in aggregated intermolecular β-sheet is accompanied by a significant decrease in α-helix. A negative cross-peak was observed at 1655–1644 cm^{-1}, as well as a positive one at 1655–1633 cm^{-1}, indicating that a decrease in α-helix was accompanied by an increase in random coil.

4. Discussion

Cytochrome *c*, apart from having an indispensable task in the electron transport chain of eukaryotes, is capable of initiating apoptosis through cardiolipin peroxidation and binding to Apaf-1 [10,18–20,56]. Many data show that cytochrome *c* and cardiolipin interacts strongly with each other, not only by electrostatic interactions but also hydrophobic ones, inducing conformational alterations in the protein [3,4,6,7,13–15,41,45]. The existence of electrostatic interactions between cytochrome *c* and the phospholipid molecules would imply a direct interaction between the protein and the phospholipid headgroups. However, the existence of hydrophobic interactions between them would also imply the

possibility that the protein could enter into the palisade structure of the membrane [5,57]. Since the interaction between cytochrome *c* and cardiolipin is so strong and it has so many implications, we have tried in this work to obtain information on the specific type of interaction between the two types of molecules and look for the specific components of secondary structure elements of the protein which might be directly implicated in binding to the phospholipid. By this way, we report the results of a study using generalized 2D-IR correlation spectroscopy to obtain synthermal spectra in order to investigate the interaction and conformation of cytochrome *c*, in both oxidized and reduced states, bound to phospholipid model membranes composed of binary mixtures of a zwitterionic phospholipid ($DMPC_d$) and a negatively charged one, either TMCL or DMPA, and compare the data between the two model biomembrane systems.

The interaction of proteins with membrane surfaces involves a number of steps, including the initial binding to the membrane, induction or stabilization of a specific secondary structure upon the interaction of the protein with the phospholipids, modulation of the phospholipid biophysical properties by binding, and finally the possible insertion of the protein in the membrane, either partially or fully. Since it has been known for a long time that the melting process of membrane phospholipids is influenced by many types of molecules including proteins, and a shift in the frequency of the CH_2/CD_2 symmetric stretching band is a reliable index of the phase behavior of phospholipid dispersions, we have made a detailed study of these stretching vibration bands in the presence of both oxidized and reduced cytochrome *c*. Moreover, we have analyzed the thermotropic behavior of the Amide I′ band of the protein in the presence of the model membrane systems to observe and relate any change in the protein with the thermotropic behavior of the phospholipids. From these data we have observed that in the binary model membrane and protein mixture there are two main transitions, one which corresponds to the phospholipid transition and another one which corresponds to protein unfolding. If there were a specific interaction between the different molecules involved, it should be possible to observe a change in the secondary structure elements of the protein involved in the interaction with the phospholipids at temperatures at which the main phospholipid transition is observed.

Our results are fully compatible with infrared data obtained by other authors [6,28,58] in which the α-helical content of the protein is about 40%, besides having some random and β-turn secondary elements. In the same way, there were no significant differences between the oxidized and reduced forms of the protein in solution. Upon increasing the temperature, there was a significant change on the Amide I′ maximum due to unfolding of the protein, decreasing the α-helical content and a concomitant increase in β-turn and random coil [6,28,29]. In all cases, the reduced form of cytochrome *c* presented a greater thermal stability than the oxidized one. There were no new secondary structure elements upon binding of cytochrome *c* to membranes, but a slight decrease in the α-helical content at the same time that a slight increase in random coil was noticed, suggesting that cytochrome *c*, when bound to the membrane surface, was more disordered than in solution. These data would suggest, in accordance with other authors, that the most significant change should be due to changes in the tertiary structure rather than on changes on secondary structure, since the denaturation temperature decreases upon membrane binding [6,7,13–15,45,59].

The binding of cytochrome *c* to membranes containing negatively-charged phospholipids, either TMCL or DMPA, but not to zwitterionic ones, was confirmed by infrared spectroscopy since the Amide I′ band corresponding to the protein was absent in membranes formed by pure $DMPC_d$. However, it should be stressed that secondary structure changes were always greater in the presence of binary mixtures composed of TMCL than in the presence of DMPA, demonstrating the specificity of binding of cytochrome *c* to cardiolipin. Interestingly, the binding of cytochrome *c* was slightly higher for mixtures containing TMCL than for mixtures containing DMPA. For oxidized cytochrome *c* in the presence of TMCL, the most intense observed Amide I′ auto-peaks were located at 1658 and 1633 cm^{-1} indicating that these are the frequencies at which the main changes in secondary structure should take place due to the interaction of the protein with the phospholipid. In the case of reduced cytochrome *c*, the auto-peaks, located at 1635 and 1621 cm^{-1}, were wider and less intense, showing, in the first place, the differences between the two redox states of the protein, and in the second one, the different secondary structures involved in the interaction, i.e., α-helix for the oxidized one and aggregated β-sheet for the reduced one. In the case of DMPA containing vesicles, the data were very similar to that obtained for reduced cytochrome *c* in the presence of TMCL, demonstrating the specific interaction of oxidized cytochrome *c* with TMCL. The data obtained at higher temperatures than those corresponding to the phase transition of the phospholipid mixtures showed that the most significant event was due to the unfolding of the protein, being similar for all redox states and mixtures assayed. In the same way, the analysis of the temperature dependence of the maximum of the Amide I′ band and the percentages of secondary structure indicate that the oxidized form of cytochrome *c* interacts strongly with cardiolipin than the reduced one [60]. These data were also reflected in the temperature dependence of the CH_2/CD_2 stretching vibrational bands of the phospholipids, since a bigger effect was observed in the negative-charged phospholipids (either TMCL or DMPA) than on the zwitterionic one ($DMPC_d$).

Using 2D-IR generalized correlation spectroscopy in order to compare the data between the two redox stated of cytochrome *c* and the two model biomembrane systems used, we found significant changes in secondary structure of oxidized cytochrome *c* in the first temperature range studied (the one pertaining to the gel to liquid-crystalline phase temperature of the phospholipid mixture), such that the α-helical component of oxidized cytochrome *c* in presence of TMCL increases in intensity (and possibly segments connecting α-helices). These data would indicate that these secondary structure elements would be in close contact with the phospholipid molecules, since the only physical change occurring at this temperature range is the phase transition. The appearance of slight

differences in β-turns and aggregation phenomena, which are also observed for the protein in solution, could be related to changes in temperature than to the specific interaction of the protein with the membrane surface. When reduced cytochrome *c* was used, an increase in random coil was observed, indicating that the interaction of both redox states with membranes was different but also that the oxidized form was more stable than the reduced one. Interestingly, in the presence of the binary mixture containing DMPA no significant differences were found between the two redox states of the protein. When the second temperature range was analyzed, no significant changes were found between the two forms of cytochrome *c* and the two phospholipid binary mixtures, since in all cases, a significant change in the α-helical content of the protein was observed. These results show that there are important differences in the secondary structure of cytochrome *c* in the presence of model membrane systems containing negatively-charged phospholipids. These differences were much more dramatic in the presence of cardiolipin than in the presence of phosphatidic acid, in accordance with published reports.

Acknowledgements

This work was supported by grant BFU2005-00186-BMC (Ministerio de Ciencia y Tecnología, Spain) to J.V. A.B is a recipient of a pre-doctoral fellowship from Ministerio de Educación, Cultura y Deporte, Spain. We also thank Drs. Morita and Ozaki for making available the 2D-Shige program for 2D-IR.

References

[1] M.M. Snel, D. Marsh, Membrane location of apocytochrome *c* and cytochrome *c* determined from lipid–protein spin exchange interactions by continuous wave saturation electron spin resonance, Biophys. J. 67 (1994) 737–745.

[2] Z. Salamon, G. Tollin, Surface plasmon resonance studies of complex formation between cytochrome *c* and bovine cytochrome *c* oxidase incorporated into a supported planar lipid bilayer. I. Binding of cytochrome *c* to cardiolipin/phosphatidylcholine membranes in the absence of oxidase, Biophys. J. 71 (1996) 848–857.

[3] M. Rytomaa, P. Mustonen, P.K. Kinnunen, Reversible, nonionic, and pH-dependent association of cytochrome *c* with cardiolipin-phosphatidylcholine liposomes, J. Biol. Chem. 267 (1992) 22243–22248.

[4] G.P. Gorbenko, J.G. Molotkovsky, P.K. Kinnunen, Cytochrome C interaction with cardiolipin/phosphatidylcholine model membranes: effect of cardiolipin protonation, Biophys. J. 90 (2006) 4093–4103.

[5] T. Heimburg, D. Marsh, Protein surface-distribution and protein–protein interactions in the binding of peripheral proteins to charged lipid membranes, Biophys. J. 68 (1995) 536–546.

[6] A. Muga, H.H. Mantsch, W.K. Surewicz, Membrane binding induces destabilization of cytochrome *c* structure, Biochemistry 30 (1991) 7219–7224.

[7] T.J. Pinheiro, The interaction of horse heart cytochrome *c* with phospholipid bilayers. Structural and dynamic effects, Biochimie 76 (1994) 489–500.

[8] F.L. Hoch, Cardiolipins and biomembrane function, Biochim. Biophys. Acta 1113 (1992) 71–133.

[9] W. Hubner, H.H. Mantsch, M. Kates, Intramolecular hydrogen bonding in cardiolipin, Biochim. Biophys. Acta 1066 (1991) 166–174.

[10] Y. Shidoji, K. Hayashi, S. Komura, N. Ohishi, K. Yagi, Loss of molecular interaction between cytochrome *c* and cardiolipin due to lipid peroxidation, Biochem. Biophys. Res. Commun. 264 (1999) 343–347.

[11] R.A. Demel, W. Jordi, H. Lambrechts, H. van Damme, R. Hovius, B. de Kruijff, Differential interactions of apo- and holocytochrome *c* with acidic membrane lipids in model systems and the implications for their import into mitochondria, J. Biol. Chem. 264 (1989) 3988–3997.

[12] T. Heimburg, P. Hildebrandt, D. Marsh, Cytochrome c-lipid interactions studied by resonance Raman and 31P NMR spectroscopy. Correlation between the conformational changes of the protein and the lipid bilayer, Biochemistry 30 (1991) 9084–9089.

[13] P.J. Spooner, A. Watts, Reversible unfolding of cytochrome *c* upon interaction with cardiolipin bilayers. 2. Evidence from phosphorus-31 NMR measurements, Biochemistry 30 (1991) 3880–3885.

[14] P.J. Spooner, A. Watts, Reversible unfolding of cytochrome *c* upon interaction with cardiolipin bilayers. 1. Evidence from deuterium NMR measurements, Biochemistry 30 (1991) 3871–3879.

[15] T.J. Pinheiro, G.A. Elove, A. Watts, H. Roder, Structural and kinetic description of cytochrome *c* unfolding induced by the interaction with lipid vesicles, Biochemistry 36 (1997) 13122–13132.

[16] N.A. Belikova, Y.A. Vladimirov, A.N. Osipov, A.A. Kapralov, V.A. Tyurin, M.V. Potapovich, L.V. Basova, J. Peterson, I.V. Kurnikov, V.E. Kagan, Peroxidase activity and structural transitions of cytochrome *c* bound to cardiolipin-containing membranes, Biochemistry 45 (2006) 4998–5009.

[17] L. Piccotti, M. Buratta, S. Giannini, P. Gresele, R. Roberti, L. Corazzi, Binding and release of cytochrome *c* in brain mitochondria is influenced by membrane potential and hydrophobic interactions with cardiolipin, J. Membr. Biol. 198 (2004) 43–53.

[18] H. Bayir, B. Fadeel, M.J. Palladino, E. Witasp, I.V. Kurnikov, Y.Y. Tyurina, V.A. Tyurin, A.A. Amoscato, J. Jiang, P.M. Kochanek, S.T. DeKosky, J.S. Greenberger, A.A. Shvedova, V.E. Kagan, Apoptotic interactions of cytochrome *c*: redox flirting with anionic phospholipids within and outside of mitochondria, Biochim. Biophys. Acta 1757 (2006) 648–659.

[19] V.E. Kagan, V.A. Tyurin, J. Jiang, Y.Y. Tyurina, V.B. Ritov, A.A. Amoscato, A.N. Osipov, N.A. Belikova, A.A. Kapralov, V. Kini, I.I. Vlasova, Q. Zhao, M. Zou, P. Di, D.A. Svistunenko, I.V. Kurnikov, G.G. Borisenko, Cytochrome c acts as a cardiolipin oxygenase required for release of proapoptotic factors, Nat. Chem. Biol. 1 (2005) 223–232.

[20] H. Iwase, T. Takatori, M. Nagao, K. Iwadate, M. Nakajima, Monoepoxide production from linoleic acid by cytochrome *c* in the presence of cardiolipin, Biochem. Biophys. Res. Commun. 222 (1996) 83–89.

[21] J.L. Arrondo, A. Muga, J. Castresana, F.M. Goni, Quantitative studies of the structure of proteins in solution by Fourier-transform infrared spectroscopy, Prog. Biophys. Mol. Biol. 59 (1993) 23–56.

[22] J.L. Arrondo, F.M. Goni, Structure and dynamics of membrane proteins as studied by infrared spectroscopy, Prog. Biophys. Mol. Biol. 72 (1999) 367–405.

[23] P. Hamm, M. Lim, W.F. DeGrado, R.M. Hochstrasser, The two-dimensional IR nonlinear spectroscopy of a cyclic penta-peptide in relation to its three-dimensional structure, Proc. Natl. Acad. Sci. U. S. A. 96 (1999) 2036–2041.

[24] I. Noda, Two-dimensional infrared spectroscopy, J. Am. Chem. Soc. 111 (1989) 8116–8118.

[25] I. Noda, Two-dimensional infrared (2D-IR) spectroscopy. Theory and applications, Appl. Spectrosc. 44 (1990) 550–561.

[26] J.L. Arrondo, X. Coto, J.C. Milicua, M. Kveder, G. Pifat, Interaction of alcohols with serum LDL An infrared study, Chem. Phys. Lipids 141 (2006) 205–215.

[27] L.M. Contreras, F.J. Aranda, F. Gavilanes, J.M. Gonzalez-Ros, J. Villalain, Structure and interaction with membrane model systems of a peptide derived from the major epitope region of HIV protein gp41: implications on viral fusion mechanism, Biochemistry 40 (2001) 3196–3207.

[28] A. Filosa, Y. Wang, A.A. Ismail, A.M. English, Two-dimensional infrared correlation spectroscopy as a probe of sequential events in the thermal unfolding of cytochromes c, Biochemistry 40 (2001) 8256–8263.

[29] M.J. Paquet, M. Laviolette, M. Pezolet, M. Auger, Two-dimensional infrared correlation spectroscopy study of the aggregation of cytochrome *c* in the presence of dimyristoylphosphatidylglycerol, Biophys. J. 81 (2001) 305–312.

[30] S. Sanchez-Bautista, A. Kazaks, M. Beaulande, A. Torrecillas, S. Corbalan-Garcia, J.C. Gomez-Fernandez, Structural study of the catalytic domain of PKCzeta using infrared spectroscopy and two-dimensional infrared correlation spectroscopy, FEBS J. 273 (2006) 3273–3286.
[31] C.S.F. Böttcher, C.M. Van Gent, C. Fries, A rapid and sensitive sub-micro phosphorus determination. Anal. Chim. Acta 1061 (1961) 203–204.
[32] H. Edelhoch, Spectroscopic determination of tryptophan and tyrosine in proteins, Biochemistry 6 (1967) 1948–1954.
[33] M. Giudici, R. Pascual, L. de la Canal, K. Pfuller, U. Pfuller, J. Villalain, Interaction of viscotoxins A3 and B with membrane model systems: implications to their mechanism of action, Biophys. J. 85 (2003) 971–981.
[34] J.K. Kauppinen, D.J. Moffatt, H.H. Mantsch, D.G. Cameron, Fourier transform in the computation of self-deconvoluted first-order derivative spectra of overlapped contours, Anal. Chem. 53 (1981) 1454–1457.
[35] D.G. Cameron, D.J Moffatt, Deconvolution, derivation, smoothing of spectra using Fourier transforms, J. Test. Eval. 12 (1984) 78–85.
[36] P.R. Griffiths, G.L Pariente, Introduction to spectral deconvolution, Trends Anal. Chem. 5 (1986) 209–215.
[37] H. Fabian, H.H. Mantsch, C.P. Schultz, Two-dimensional IR correlation spectroscopy: sequential events in the unfolding process of the lambda cro-V55C repressor protein, Proc. Natl. Acad. Sci. U. S. A. 96 (1999) 13153–13158.
[38] M. Jackson, H.H. Mantsch, The use and misuse of FTIR spectroscopy in the determination of protein structure, Crit. Rev. Biochem. Mol. Biol. 30 (1995) 95–120.
[39] T. Lefevre, K. Arseneault, M. Pezolet, Study of protein aggregation using two-dimensional correlation infrared spectroscopy and spectral simulations, Biopolymers 73 (2004) 705–715.
[40] H.H. Mantsch, R.N. McElhaney, Phospholipid phase transitions in model and biological membranes as studied by infrared spectroscopy, Chem. Phys. Lipids 57 (1991) 213–226.
[41] A. Muga, H.H. Mantsch, W.K. Surewicz, Apocytochrome *c* interaction with phospholipid membranes studied by Fourier-transform infrared spectroscopy, Biochemistry 30 (1991) 2629–2635.
[42] M.B. Sankaram, G.L. Powell, D. Marsh, Effect of acyl chain composition on salt-induced lamellar to inverted hexagonal phase transitions in cardiolipin, Biochim. Biophys. Acta 980 (1989) 389–392.
[43] P. Garidel, C. Johann, A. Blume, Nonideal mixing and phase separation in phosphatidylcholine-phosphatidic acid mixtures as a function of acyl chain length and pH, Biophys. J. 72 (1997) 2196–2210.
[44] L.M. Contreras, R.F. de Almeida, J. Villalain, A. Fedorov, M. Prieto, Interaction of alpha-melanocyte stimulating hormone with binary phospholipid membranes: structural changes and relevance of phase behavior, Biophys. J. 80 (2001) 2273–2283.
[45] T. Heimburg, D. Marsh, Investigation of secondary and tertiary structural changes of cytochrome *c* in complexes with anionic lipids using amide hydrogen exchange measurements: an FTIR study, Biophys. J. 65 (1993) 2408–2417.
[46] W.K. Surewicz, H.H. Mantsch, New insight into protein secondary structure from resolution-enhanced infrared spectra, Biochim. Biophys. Acta 952 (1988) 115–130.
[47] D.M. Byler, H. Susi, Examination of the secondary structure of proteins by deconvolved FTIR spectra, Biopolymers 25 (1986) 469–487.
[48] W.C. Reisdorf Jr, S. Krimm, Infrared amide I′ band of the coiled coil, Biochemistry 35 (1996) 1383–1386.
[49] S.T. Walsh, R.P. Cheng, W.W. Wright, D.O. Alonso, V. Daggett, J.M. Vanderkooi, W.F. DeGrado, The hydration of amides in helices; a comprehensive picture from molecular dynamics, IR, and NMR, Protein Sci. 12 (2003) 520–531.
[50] G.W. Bushnell, G.V. Louie, G.D. Brayer, High-resolution three-dimensional structure of horse heart cytochrome *c*, J. Mol. Biol. 214 (1990) 585–595.
[51] T. Takano, R.E. Dickerson, Conformation change of cytochrome *c*. I. Ferrocytochrome *c* structure refined at 1.5 A resolution, J. Mol. Biol. 153 (1981) 79–94.
[52] L. Banci, I. Bertini, K.L. Bren, H.B. Gray, P. Sompornpisut, P. Turano, Solution structure of oxidized *Saccharomyces cerevisiae* iso-1-cytochrome *c*, Biochemistry 36 (1997) 8992–9001.
[53] R. Sanishvili, K.W. Volz, E.M. Westbrook, E. Margoliash, The low ionic strength crystal structure of horse cytochrome *c* at 2.1 A resolution and comparison with its high ionic strength counterpart, Structure 3 (1995) 707–716.
[54] T. Takano, R.E. Dickerson, Redox conformation changes in refined tuna cytochrome *c*, Proc. Natl. Acad. Sci. U. S. A. 77 (1980) 6371–6375.
[55] A. Filosa, A.M. English, Probing local thermal stabilities of bovine, horse, and tuna ferricytochromes c at pH 7, J. Biol. Inorg. Chem. 5 (2000) 448–454.
[56] J. Cai, J. Yang, D.P. Jones, Mitochondrial control of apoptosis: the role of cytochrome *c*, Biochim. Biophys. Acta 1366 (1998) 139–149.
[57] S. Oellerich, H. Wackerbarth, P. Hildebrandt, Conformational equilibria and dynamics of cytochrome *c* induced by binding of sodium dodecyl sulfate monomers and micelles, Eur. Biophys. J. 32 (2003) 599–613.
[58] J.F. Calvert, J.L. Hill, A. Dong, Redox-dependent conformational changes are common structural features of cytochrome *c* from various species, Arch. Biochem. Biophys. 346 (1997) 287–293.
[59] P.J. Spooner, A. Watts, Cytochrome c interactions with cardiolipin in bilayers: a multinuclear magic-angle spinning NMR study, Biochemistry 31 (1992) 10129–10138.
[60] I.L. Nantes, M.R. Zucchi, O.R. Nascimento, A. Faljoni-Alario, Effect of heme iron valence state on the conformation of cytochrome *c* and its association with membrane interfaces. A CD and EPR investigation, J. Biol. Chem. 276 (2001) 153–158.